Organic Process Research & Development

ARTICLE

pubs.acs.org/OPRD

In Situ Monitoring of Supersaturation and Polymorphic Form of Piracetam during Batch Cooling Crystallization

Mark Barrett,[†,‡] Hongxun Hao,[†,‡] Anthony Maher,[†,§] Kieran Hodnett,[†,§] Brian Glennon,[†,‡] and Denise Croker*[,†,§]

[†]Solid State Pharmaceutical Cluster (SSPC) and [‡]The School of Chemical and Bioprocess Engineering, University College Dublin, Belfield, Dublin 4, Ireland

[§]Materials and Surface Science Institute, Chemical and Environmental Science Department, University of Limerick, Ireland

Supporting Information

ABSTRACT: In situ Raman spectroscopy, infrared spectroscopy, and focused beam reflectance measurement (FBRM) were used simultaneously to monitor the polymorphic form, supersaturation profile, and chord length distribution, respectively, during a cooling crystallization of piracetam in ethanol. At fast cooling rates and fast generation of supersaturation, the metastable polymorph was observed to nucleate and prevail. On slow cooling, only the stable polymorph was observed. This was attributed to the time available to the system to respond to the generated supersaturation. If sufficient time is allowed, the system will arrange itself into its most stable thermodynamic configuration, and the stable polymorph will be produced. At fast cooling rates, the system is suject to kinetic control, resulting in crystallisation of the less stable polymorph.

INTRODUCTION

Crystallization is routinely used for purification and separation purposes across many industries, including the manufacture of pharmaceuticals. Crystallization in a polymorphic system is complicated by the possibility of nucleating different crystal forms from the same solution. Polymorphism is a well-recognized phenomenon whereby a pure chemical compound may exist in two or more structural orientations. As different polymorphs display individual physical properties such as density, melting point, and solubility, polymorphism is vitally important to the manufacture of chemicals and, in particular, pharmaceuticals. Production of an unwanted polymorph will give a product that most likely will not satisfy the intended purpose, or processing characteristics, of the required polymorph.

Several online methods, such as Raman spectroscopy, FBRM (focused beam reflectance measurement) and FTIR (Fourier transform infrared spectroscopy), can be used for in situ monitoring of the isolation and transformation of polymorphs. Raman spectroscopy is a light-scattering technique wherein a monochromatic laser source illuminates the sample, and the resulting scattered light is collected and analyzed. Raman spectroscopy has the capability to monitor both the liquid phase and the solid phase at the same time. In the research of the polymorphic transformation of mannitol,[1,2] L-glutamic acid,[3,4] carbamazepine,[5] and *p*-aminobenzoic acid,[6] Raman showed good applicability as an in situ tool. FBRM is a probe-based high solids concentration particle characterization tool and can obtain particle dimension measurements over a large size range. Dang et al.[7] have used FBRM to monitor the polymorphic transformation from the β to the α form of glycine, while O'Sullivan et al.[8] combined FBRM with FTIR in researching the transformation process from δ- to β-mannitol.

Attenuated total reflectance Fourier transform infrared (ATR-FTIR) spectroscopy has emerged as the primary instrument for the assessment of bulk supersaturation during both cooling and antisolvent crystallization processes. Early work presented techniques for supersaturation assessment which linked temperature and spectral values, through basic polynomial expressions, to the correlation of solute and solvent peak heights. Much research since then has also focused on advanced chemometric calibration models, such as partial least-squares (PLS). Recently, however, a novel calibration-free method for in situ monitoring of supersaturation during the crystallization process was described by Barrett et al.[9] This method was successfully used to monitor the crystallization process of benzoic acid and one kind of active pharmaceutical ingredient (API).

Piracetam is a polymorphic drug compound. Five polymorphic forms of piracetam have been reported, but two of these (FIVand FV) are obtained only in high-pressure (>0.5 GPa) conditions.[10] The reaming polymorphs, FI, FII, and FIII, have been identified and structurally characterized under ambient conditions.[11,12] FI is highly unstable and can be isolated only by heating FII or FIII to 400 K and then quenching to room temperature. It transforms back to FII within a few hours and thus is not of much practical relevance. FII is metastable, and FIII is the stable polymorph, as determined by melting points. FI and FIII are enantiotropically related, with a transition temperature at 75 °C. Kuhnert Brandstatter et al. claim that FII and FIII also have an enantiotropic relationship with a transition temperature at greater than 75 °C, but no experimental evidence exists to verify this. The solubility of FIII has been determined by Maher et al.[13] The cooling crystallization of piracetam from different saturated solvent systems has been previously described in literature. Pavlova et al. reported isolation of FIII from methanol and ethanol, FII from *n*-butanol, *p*-dioxane, acetonitrile, and

Received: March 14, 2011
Published: April 28, 2011

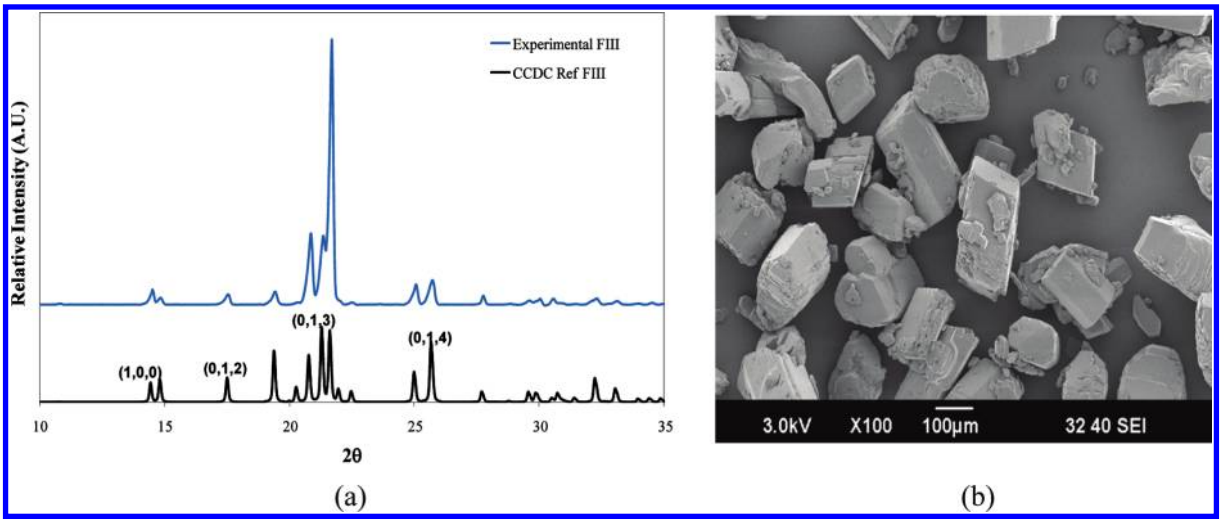

Figure 1. (a) Powder X-ray diffraction pattern of solids recovered from the preparation of the FII polymorph of piracetam; (b) corresponding scanning electron micrograph.

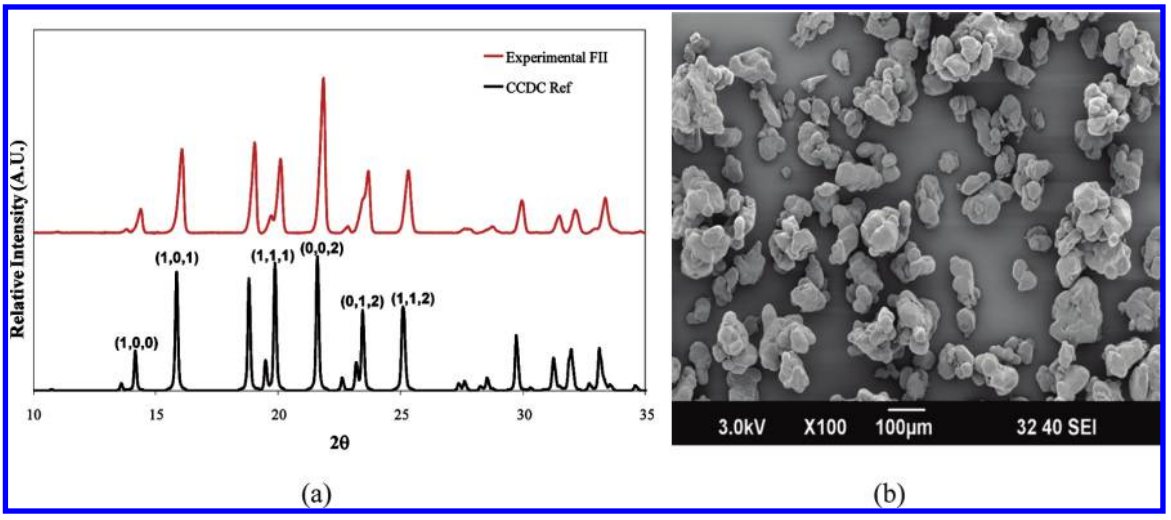

Figure 2. (a) Powder X-ray diffraction pattern of solids recovered from the preparation of the FIII polymorph of piracetam; (b) corresponding scanning electron micrograph.

chloroform, and FI from 1,2-diacetoxyethane but gives little experimental detail.[14] More recently, Dematos et al. monitored the crystallization of piracetam form methanol, 2-propanol, isobutanol, and nitromethane using an in situ energy dispersive X-ray diffraction method.[15] In this study, all three polymorphs were identified during the cooling crystallization. FI formed initially but had a short lifetime and transformed to FII and/or FIII with continued cooling.

The objective of this work is to use in situ Raman spectroscopy to monitor the polymorphic form of the product formed from a cooling crystallization of piracetam in ethanol. The effect of the rate of generation of supersaturation on the polymorphic product will also be demonstrated by varying the cooling rate.

EXPERIMENTAL SECTION

Polymorph Preparation. Piracetam was supplied by AXO Industry Ltd. and complies with European Pharmacopoeia standards (CAS number: 7491-74-9). Ethanol was reagent grade.

The FIII polymorph of piracetam was produced from a cooling crystallization in methanol; 336 g of the commercial product was dissolved in 700 g of methanol at 60 °C in a Mettler-Toledo Labmax 1-L reactor over 2 h. The solution was cooled at 0.1 °C min^{-1} to 20 °C, agitated for 4 h, and cooled further at 0.1 °C min^{-1} to 5 °C and agitated for a further 10 h. The solids were isolated over a 0.22 μm PVDF membrane using vacuum filtration, washed with a small amount of propanol, and held at 55 °C overnight to dry. The FII polymorph of piracetam was produced by subjecting the prepared FIII to heat treatment. Ten grams of FIII was ground to a fine powder and placed in an oven at 140 °C for 3 days, with occasional stirring. The powder was removed from the oven and allowed to return to room temperature where it was held for 5 days. The FI polymorph was not considered in this study due to reasons of stability. Pure FI solid could not be maintained long enough to record a reference Raman spectrum.

Powder X-ray diffraction (PAN analytical X'Pert MPD PRO) was used to confirm polymorphic purity for both forms, and the

dx.doi.org/10.1021/op2000628 |Org. Process Res. Dev. 2011, 15, 681–687

powders were imaged using scanning electron microscopy (Joel Carryscope JCM-5700).

Crystallization Methodology. A 100-mL Mettler-Toledo Easymax system was used in conjunction with the iControl software platform for all crystallization experiments. A Kaiser Raman RXN2 system was used to measure the Raman spectra of different samples. This system contains a Kaiser Invictus laser emitting deep-red and nearly invisible (785 nm) emission of 450 mW. The spectral range of this system is from 100 to 1890 cm^{-1}, the spectral resolution is 5 cm^{-1} average. The MR probe head with immersion optics was used to monitor the polymorphs of piracetam in situ in solution. The iC Raman software (Mettler-Toledo) is used for instrument configuration, data acquisition, and data analysis.

Both the FBRM and ATR-FTIR technologies used in this paper were manufactured by Mettler-Toledo. The FBRM (model S400A) measurement duration was set at 10 s. Weighted and unweighted chord length distribution (CLD) data were used to monitor the size distribution of different products. iC FBRM software was used during the experiment to collect and analyze the data. The ATR-FTIR (model iC 10, DiComp probe with AgX halide fiber) measurement duration was also set at 15 s, and spectra were collected from 100 to 1890 cm^{-1}. iC IR software was used to collect and analyze the data.

Slow (0.1 °C/min), fast (1 °C/min), and crash (3.5 °C/min) cooling rates from 50 to 10 °C were assessed for the crystallization. The crash cooling rate was selected to push the system to nonequilibrium as fast as possible. A saturated (with respect to FIII) solution of piracetam in ethanol at 40 °C was prepared by adding 3.17 g of FIII to 40 g of ethanol. The solution was heated to 50 °C for 15 min to ensure complete dissolution. The required cooling rate was applied, and the solution was maintained at 10 °C for 10 min.

A 125−250 μm sieve fraction of the pure FIII polymorph as produced above was used as seed. The following seed loadings were investigated: high (5% of the solids loaded in the saturated solution), medium (1%), and low (0.5%). The purpose of seeding was not to control particle size but to direct nucleation of the desired polymorphic form. A constant cooling rate of 1°C/min was applied for each seeded crystallization. The solution was cooled to 35 °C (with 5 °C inside the solubility curve) for seed addition; a hold time of 30 min was applied before cooling was continued to 10 °C.

RESULTS

Preparation of the Pure Polymorphs. Powder X-ray diffraction analysis confirmed the production of both the pure FII and FIII polymorphs (Figures 1 and 2, respectively). Scanning electron microscopy demonstrated the habit of each of the produced polymorphs. The irregular habit of FII is due to the preparation method (heat treatment).

Identification of the Polymorphs Using Raman Spectroscopy. Raman spectroscopy offers a fingerprint for different compositions and solid-state forms. Different polymorphs of the same compound have different packing of molecules, and so the Raman spectra of different polymorphs will be different due to different molecular vibrations and rotations. The Raman spectra (from 250 cm^{-1} to 1890 cm^{-1}) of FII and FIII of piracetam are shown in Figure 3. It can be seen that there are small differences between the Raman spectra of these two forms. In the spectral range of 1620−1680 cm^{-1}, FII has one characteristic peak at 1653 cm^{-1}, whereas FIII has one characteristic peak at 1649 cm^{-1}. The difference is shown clearly in Figure 4 and was used to monitor the different polymorphs of piracetam in situ during the cooling crystallization.

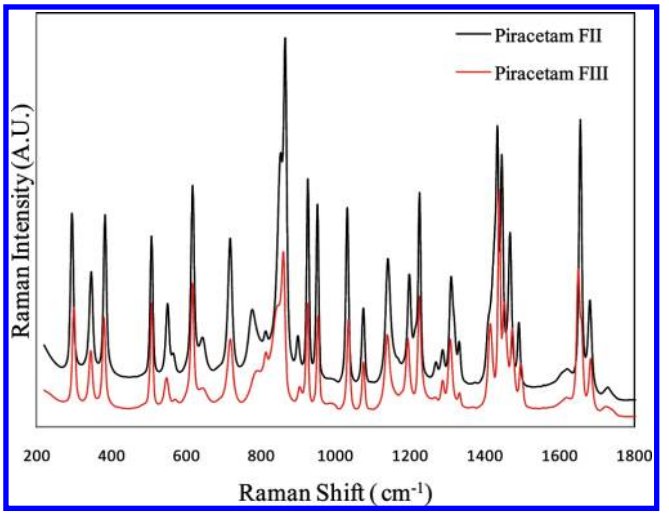

Figure 3. Raman spectra of pure FII and pure FIII polymorphs of piracetam.

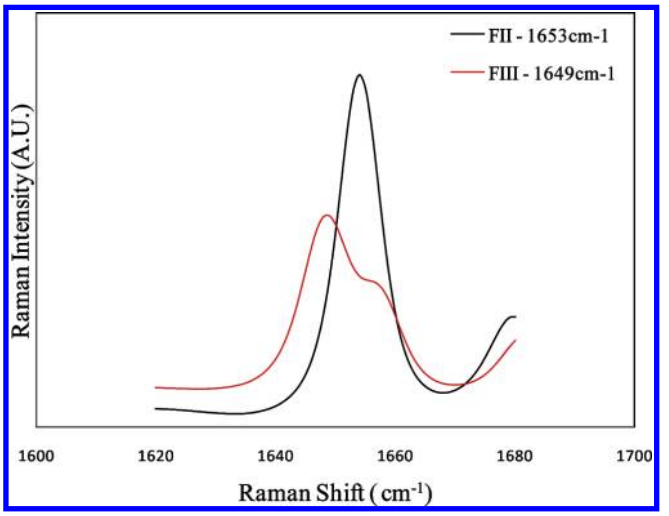

Figure 4. Raman spectra (1620−1680 cm^{-1}) recorded for pure FII and pure FIII polymorphs of piracetam.

Expressing Solubility in Terms of ATR-FTIR Peak Area. The spectra recorded for pure ethanol and a saturated solution of piracetam in ethanol at 40 °C, using the ATR-FTIR probe, are presented in Figure 5. The peak at ∼1700 cm^{-1} is specific to piracetam and is due to stretching of the carbonyl bond in the molecule. The peak at ∼1050 cm^{-1} is due to the C−O bond in ethanol and was used as a reference peak. The concentration of piracetam was monitored in situ using a ratio of the peak area of each peak as per eq 1. Peak areas were calculated automatically from the iC IR software platform, using the peak area to 2-point baseline function.

$$\text{peak area ratio} = \text{piracetam (1694 cm}^{-1}\text{) peak area/ethanol (1047 cm}^{-1}\text{) peak area} \quad (1)$$

A solution containing 3.17 g of FIII piracetam and 40 g of ethanol (saturation temperature = 40 °C) was prepared at 10 °C and heated at 0.1 °C/min to 50 °C to determine the solubility

dx.doi.org/10.1021/op2000628 |Org. Process Res. Dev. 2011, 15, 681–687

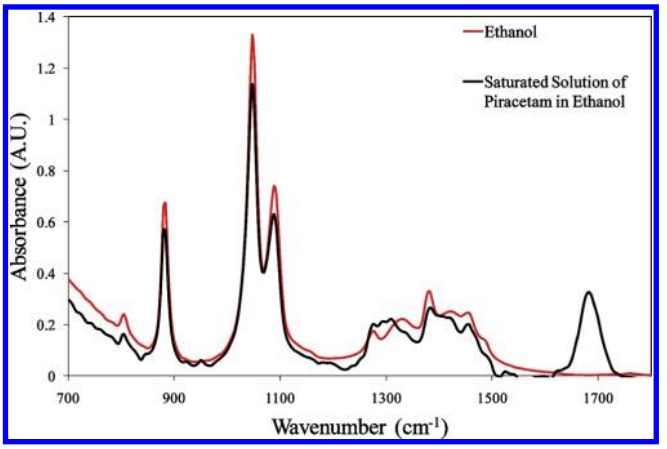

Figure 5. Mid-IR spectra (700−1800 cm $^{-1}$) recorded for ethanol and a saturated solution of piracetam in ethanol (at 40 °C), using the ATR FTIR probe.

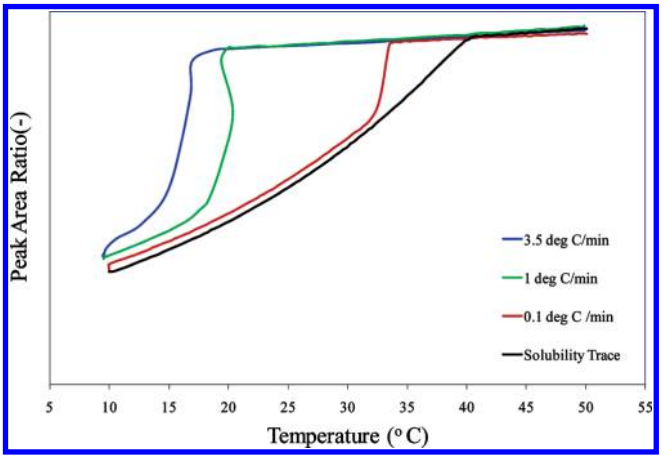

Figure 6. Solubility curve and supersaturation trajectory, in terms of peak area ratio, obtained from the cooling crystallization of a solution of piracetam in ethanol, saturated at 40 °C, as a function of cooling rate.

curve of the FIII polymorph of piracetam as a function of the peak area ratio and temperature. An increase in the peak area ratio was observed up to 40 °C at which point it reached a plateau, corresponding with complete dissolution of the solid content (Figure 6, black line). This curve provided a representation of the solubility curve of piracetam in ethanol in terms of peak area and was used to monitor supersaturation in subsequent crystallization experiments.[1,9] This procedure was also attempted for the FII polymorph, but this form tended to transform to FIII as it was heated up, preventing measurement of an accurate solubility curve for FII. In an effort to illustrate the magnitude of the solubility difference between FII and FIII, a gravimetric method of solubility determination was attempted. The solubility of FII and FIII was measured respectively as 0.035 and 0.032 g/g of ethanol at 20 °C using gravimetric analysis, but this will be further explored in a forthcoming publication.

The Effect of Cooling Rate on Supersaturation and Polymorphic Form. The concentration of dissolved piracetam was monitored in situ during the cooling crystallization, and is expressed in Figure 6 in terms of the peak area ratio described above. The peak area ratio remains constant until nucleation, at which point a sudden

Table 1. Observed nucleation temperature, metastable zone width (MSZW), polymorphic form, and calculated supersaturation for the cooling crystallization of a saturated solution of piracetam in ethanol, as a function of cooling rate

cooling rate (°C/min)	nucleation temperature (°C)	MSZW (°C)	supersaturation	polymorphic form
3.5	18.2	21.8	1.4	FII
1	20.4	19.6	1	FII
0.1	33.5	6.5	0.26	FIII

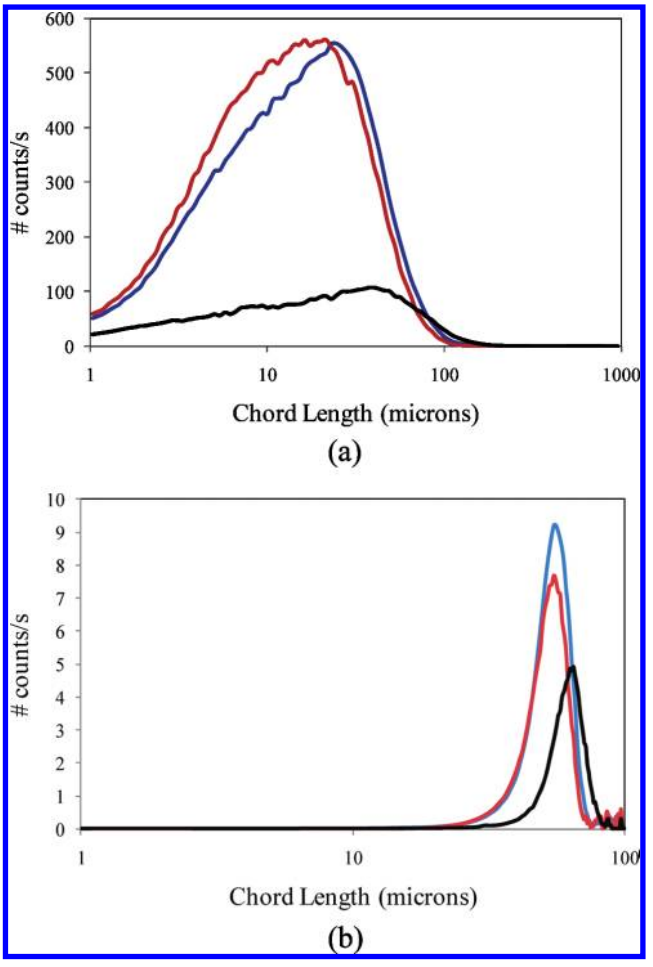

Figure 7. Unweighted (a) and square weighted (b) FBRM chord length distributions resulting from cooling a saturated solution of piracetam in ethanol, as a function of cooling rate: (blue) crash cool, (red) fast cool, (black) slow cool.

decrease in the peak area ratio is observed as a result of the removal of solute from solution. The metastable zone width is measured from the solubility curve to the point of nucleation (Table 1). A peak area ratio in excess of the equilibrium peak area ratio indicates supersaturation and allows for the calculation of absolute supersaturation (S) using eq 2, where PA_T represents the peak area ratio at a given temperature, T, and PA_T^* represents the equilibrium peak area ratio at that temperature (Table 1). This supersaturation is specific to the FIII polymorph. As the FII polymorph is less stable

dx.doi.org/10.1021/op2000628 |Org. Process Res. Dev. 2011, 15, 681–687

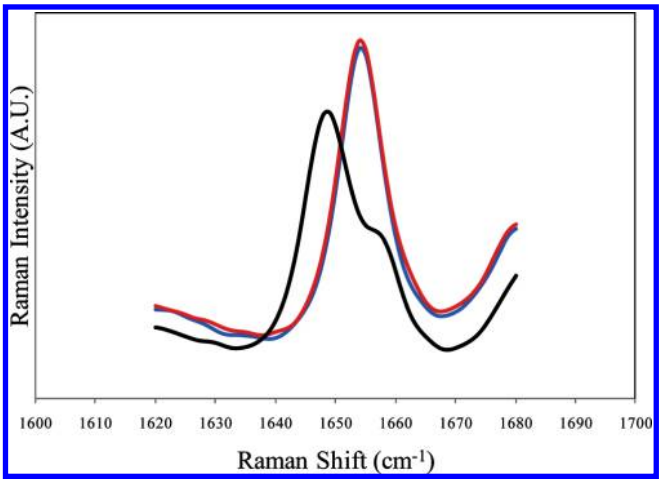

Figure 8. Raman spectra (1620−1680 cm^{-1}) recorded for the crystallization of a saturated solution of piracetam in ethanol, as a function of cooling rate.

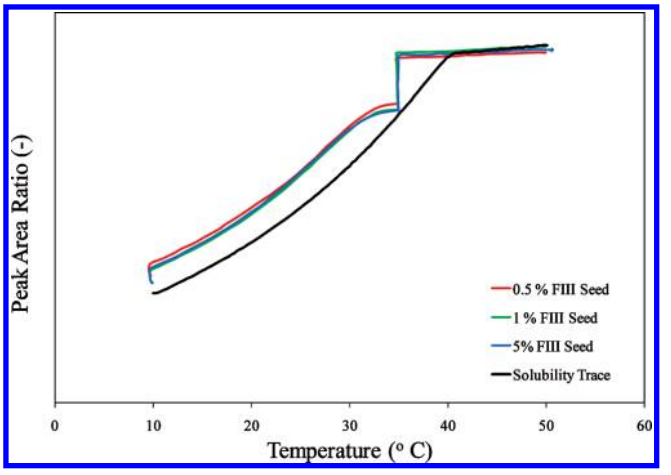

Figure 9. Supersaturation trajectory, in terms of peak area ratio, obtained for cooling crystallization (1 °C/min) of a solution of piracetam in ethanol saturated at 40 °C, in the presence of different seed amounts of the FIII polymorph.

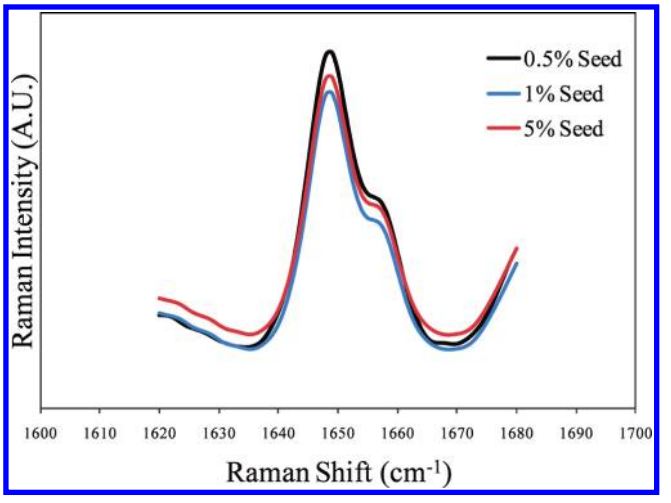

Figure 10. Raman spectra (1620−1680 cm^{-1}) recorded for the seeded crystallization of a saturated solution of piracetam in ethanol, as a function of the amount of FIII seed added.

than FIII, we can presume it has a higher solubility and hence would experience a reduced degree of supersaturation relative to that of FIII.

$$S = [PA_T - PA^*_T]/PA^*_T \quad (2)$$

Fast cooling rates resulted in wider metastable zones and a higher supersaturation at nucleation than did the slow cool-down experiment, as expected. A slight increase in temperature was noted after nucleation in these experiments; this is due to the corresponding heat of crystallization. Following nucleation, the concentration decreased continuously until the isolation temperature was reached. A continuous increase in the number of fine chord lengths was recorded during cool down, with little or no shift to increased size in the chord length distribution. This suggests continuous nucleation during cooling, with little or no growth, as evidenced by the large number of fine particles in the final product size distribution (Figure 7).

The slow cool down resulted in a much narrower metastable zone and nucleation at a lower supersaturation. After nucleation the concentration reduced to the equilibrium value, with subsequent cooling generating minimum supersaturation. The desupersaturation profile closely followed the solubility curve, conditions likely to promote particle growth. The final product chord length distribution reflected this, with a smaller number of larger chord lengths recorded for the fast cooling experiments. Furthermore, the reduction in the bulk supersaturation during the slow cooling process produces notably less fine chord counts (Figure 7). This is indicative of a reduction in the nucleation rate for this process, or potentially a change in crystal habit or crystallization of a polymorphic form.

The polymorphic form at the point of nucleation was successfully identified in situ with the Raman probe (Figure 8). The metastable FII polymorph was detected during the fast cool down, while the FIII polymorph resulted from the slow cool down. A mix of polymorphic forms was not detected in either experiment. It is acknowledged that less than 5% polymorphic impurity would most likely not be detected with the Raman method. A slight delay was apparent between the point of nucleation and the response of the Raman probe at slow cooling rates. This was due to the time required for sufficient solids to accumulate in solution. Off-line X-ray diffraction measurements of solids recovered at the end of crystallization corresponded with the Raman results with respect to pure polymorphic form. The short hold time (10 min) at the end of the cool down, was selected so as to minimize the potential for solution-mediated polymorphic transformation to occur after nucleation.

At fast cooling rates, this nucleation is under kinetic control, and the metastable form is favored. At slow cooling rates, the crystallization proceeds under thermodynamic control, and the stable form is produced. This result is in good agreement with a recent study by He et al.,[16] where nucleation of the metastable form of *m*-hydroxybenzoic acid and *o*-aminobenzoic acid was reported at high rates of supersaturation generation. Can the stable polymorph be produced at a faster cooling rate if seeding is used to direct polymorph form? This was investigated by repeating the fast cooling (1 °C/min) in the presence of FIII seed.

The Use of Seeding to Direct Polymorphic Form at Fast Cooling Rates. As before, the concentration was monitored in situ for the duration of the cool down, and the resulting supersaturation

dx.doi.org/10.1021/op2000628 |*Org. Process Res. Dev.* 2011, 15, 681–687

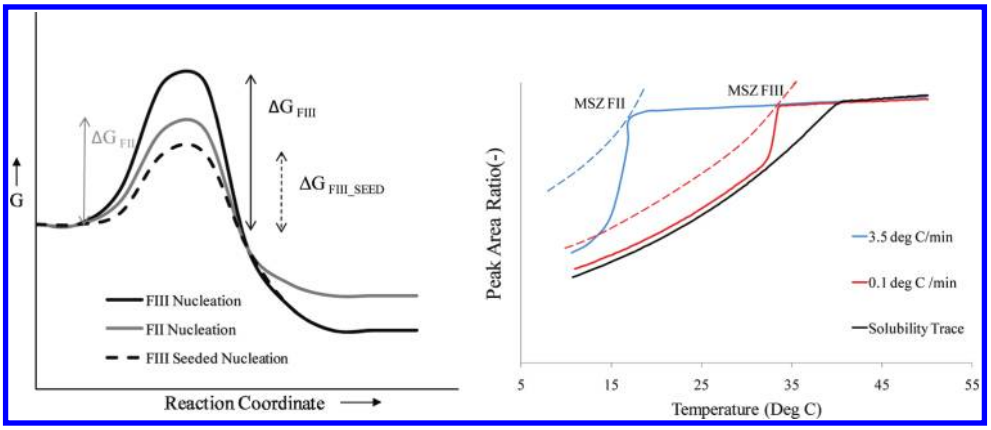

Figure 11. Schematic illustration of the energy barrier to polymorph nucleation in the above experiments. Also shown is the metastable zone observed for nucleation of the FII polymorph (at fast cooling rate) and the FIII polymorph (at slow cooling rate).

profiles are presented in Figure 9. At the point of seeding the supersaturation in solution was approximately 0.16. The addition of seed resulted in a decrease in supersaturation, with the concentration of piracetam in solution returning to the solubility curve of FIII during the 30-min hold time, regardless of seed loading. This was due to a combination of some seed growth but mainly the inducement of nucleation in the solution as indicated by a sudden increase in the fine chord length counts detected with FBRM. Subsequent cooling resulted in continued nucleation of FIII, due to the fast cooling rate. As nucleation was the primary consumer of supersaturation, the amount of seed used did not have a significant effect on the final chord length distribution; a similar result was observed for each seed loading, −0.5, 1, and 5%.

The Raman spectra produced correspond to pure FIII, indicating only FIII nucleated in the presence of the seed (Figure 10), independent of seed loading. This shows that even a small amount of FIII seed is sufficient to direct nucleation of the stable FIII polymorphs. Efforts were made to "force" nucleation of FII in the presence of FIII seed. Increasing the cooling rate alone did not result in nucleation of FII. A combination of a reduction in the seed addition temperature to 28 °C, 12 °C inside the solubility curve, no hold time, and a crash cooling rate were required to nucleate FII in the presence of FIII (see Supporting Information for relevant data).

Seeding did not have any effect on the final product size distribution (as indicated by FRBM chord lengths). This is due to two factors: the seed size was too large to provide a sufficient surface area to consume supersaturation at this cooling rate, and the cooling rate was too fast to allow growth. This could be optimized by looking at different seed sizes but was outside the scope of this study.

DISCUSSION

The rate of cool down directly controls the generation of supersaturation during a cooling crystallization, and the rate of generation of supersaturation is a controlling factor in the polymorphic composition of the resulting product. In this study the FII polymorph of piracetam was produced at fast cooling rates, and the stable FIII polymorph was produced with a slow cooling rate. The fast cool down resulted in a rapid accumulation of supersaturation in the solution. Assuming the solubility of both polymorphs is similar (as is the case in most polymorphic systems), a driving force exists for nucleation of either polymorph at this point. Nucleation of the metastable FII polymorph may be rationalized by considering the energy profile for polymorphic crystallization (Figure 11). The lowest energy barrier to nucleation exists for the metastable form, even though the overall reduction in energy is less for this form. When a system is highly supersaturated, it is far from equilibrium and will take the lowest energy option possible to relieve that supersaturation—in this case nucleation of FII. The nucleation of the stable polymorph is kinetically hampered; even though the driving force exists for nucleation of the stable phase, the system does not have sufficient time to arrange molecules in their most stable form. The metastable zone is quite large in this case as the cooling rate surpasses the system's ability to relieve supersaturation as it is generated. The cooling times prior to nucleation (taken from the point of saturation, 40 °C) were 6 and 20 min for 3.5 °C min^{-1} and 1 °C min^{-1}, respectively. When the cooling rate is reduced, supersaturation is generated more gradually. A driving force exists for nucleation of either polymorph, but the system now has additional time to arrange molecular configurations and overcome the energy barrier for nucleation of the stable phase. At 1 °C min^{-1}, 65 min passed before nucleation occurred. The system is under thermodynamic control, and the kinetic factors which resulted in FII nucleation in the previous experiment are less important. Nucleation is observed at a higher temperature corresponding to a much narrower metastable zone.

By seeding with the stable form, the energy barrier for nucleation of this form is significantly reduced, as there is now an available surface to assist nucleation of FIII. The addition of FIII seed at 35 °C induced nucleation of FIII at a temperature higher than that observed for free nucleation. The presence of an available surface has been known to significantly reduce the supersaturation required for nucleation,[17] as represented in Figure 11. This allowed for isolation of a pure FIII product within a much shorter time scale than that observed for free nucleation. The seed loading used did not have any effect on the polymorphic content of the crystallization product, even at low seed loading. FII could be forced to nucleate in the presence of the FIII seed in very highly supersaturated conditions, an observation which supports the proposal that kinetics will prevail when a system is far from equilibrium.

CONCLUSIONS

The polymorphic content of the product of a cooling crystallization for a solution of piracetam in ethanol was successfully monitored using in situ Raman spectroscopy. The corresponding

supersaturation profile was simultaneously tracked using in situ infrared spectroscopy. Rapid generation of supersaturation was found to result in nucleation and growth of the metastable FII polymorph of piracetam. Slow cooling and a low level of supersaturation favored nucleation and growth of the stable FIII polymorph. This link between supersaturation generation and polymorph product could be exploited to control the polymorph purity of the product in industrial-scale crystallization. These in situ tools offer valuable insight into crystallization mechanisms and maximize the information which can be obtained from a single experiment.

■ ASSOCIATED CONTENT

Supporting Information. X-ray diffraction patterns of the solids recovered from the crystallization experiments, Supersaturation trajectory and the peak area of the characteristic Raman peak for each polymorph when seeding was delayed until 28 °C. This material is available free of charge via the Internet at http://pubs.acs.org.

■ AUTHOR INFORMATION

Corresponding Author
*denise.croker@ul.ie Tel: +353-61-234166.

■ ACKNOWLEDGMENT

This material is based upon works supported by the Science Foundation Ireland under Grant 07/SRC/B1158.

■ REFERENCES

(1) Hao, H.; Su, W.; Barrett, M.; Caron, V.; Healy, A.-M.; Glennon, B. *Org. Process Res. Dev.* **2010**, *14* (5), 1209–1214.
(2) Su, W.; Hao, H.; Barrett, M.; Glennon, B. *Org. Process Res. Dev.* **2010**, *14* (6), 1432–1437.
(3) Qu, H.; Alatalo, H.; Hatakka, H.; Kohonen, J.; Louhi-Kultanen, M.; Reinikainen, S. P.; Kallas, J. *J. Cryst. Growth* **2009**, *311*, 3466.
(4) Scholl, J.; Bonalumi, D.; Vicum, L.; Mazzotti, M.; Muller, M. *Cryst. Growth Des.* **2006**, *6*, 881.
(5) Liu, W.; Wei, H.; Black, S. *Org. Process Res. Dev.* **2009**, *13*, 949.
(6) Yang, X.; Wang, X.; Ching, C. *J. Raman Spectrosc.* **2009**, *40*, 870.
(7) Dang, L.; Yan, H.; Black, S.; Wei, H. *Org. Process Res. Dev.* **2009**, *13*, 1301.
(8) O' Sullivan, B.; Glennon, B. *Org. Process Res. Dev.* **2005**, *9* (6), 884–889.
(9) Barrett, M.; McNamara, M.; Hongxun, H.; Barrett, P.; Glennon, B. *Chem. Eng. Res. Des.* **2010**, *88* (8), 1108–1119.
(10) Fabbiani, F. P. A.; Allan, D. R.; Parsons, S.; Pulham, C. R. *CrystEngComm* **2005**, *7*, 179–186.
(11) Pavlova, A. *Pharmazie* **1979**, *34*, 449–450.
(12) Kuhnert-Brandstaetter, M.; Burger, A.; Voellenkelee, R. *Sci. Pharm.* **1994**, *62* (3), 307–316.
(13) Maher, A.; Croker, D.; Rasmuson, A. C.; Hodnett, B. K. *J. Chem. Eng. Data* **2010**, *55* (11), 5314–5318.
(14) Pavlova, A.; Konstantinova, N.; Dashkalov, H.; Georgiev, A. *Pharmazie* **1983**, *38* (9), 634.
(15) Dematos, L.; Williams, A.; Booth, S.; Petts, C.; Taylor, D.; Blagden, N. *J. Pharm. Sci.* **2007**, *96*, 1069–1078.
(16) He, G.; Wong, A. B. H.; Chow, P. S.; Tan, R. B. H. *J. Cryst. Growth* **2011**, *314* (1), 220–226.
(17) Croker, D.; Hodnett, B. K. *Cryst. Growth Des.* **2010**, *10* (6), 2806–2816.